

Research Paper

# Horizontal Resistance Characteristics of Batter-Coupled Spiral Piles under Monotonic and Cyclic Loading

T. Kurokawa<sup>1</sup>, Y. Ide<sup>2</sup>, N. Yasufuku<sup>3</sup>, and M. Nagata<sup>4</sup>

## ARTICLE INFORMATION

### Article history:

Received: 21 September, 2023

Received in revised form: 18 December, 2023

Accepted: 24 December, 2023

Publish on: 7 February, 2024

### Keywords:

Spiral pile

Coupled piles structure

Model test

Horizontal resistance

Cyclic horizontal loading test

## ABSTRACT

Spiral piles have high axial resistance and are used as foundations for small structures. On the other hand, spiral piles have a lower bending rigidity than steel pipe piles of the same diameter, resulting in a problem of lower horizontal resistance. The authors have focused on a two-pile coupled pile structure with spiral piles, which is also resistant to horizontal forces, and have conducted research to understand its resistance characteristics. In this study, model tests were mainly conducted on coupled piles with two spiral piles as batter piles to understand their horizontal resistance characteristics. Monotonic loading tests on a dense dry sand showed that the use of spiral piles as batter piles provided higher elastic limit spring rigidity and horizontal yield load than single piles or vertically-coupled piles. Furthermore, the highest elastic limit spring rigidity was obtained when the angle of inclination of the batter pile was 45°. The durability of the batter piles under the sand conditions of this study was demonstrated by cyclic loading tests at a load equivalent to the horizontal yield load.

## 1. Introduction

Spiral piles (Fig. 1) have the advantages of no earth removal, short construction time, and low cost. Typically, spiral piles are used as foundations for relatively small structures such as agricultural greenhouses and solar power generation systems. Spiral piles are characterized by their ability to rotational driving into the ground along their twisted shape without disturbing the surrounding sand. Therefore, when the rotation of the pile body is fixed, the pile exhibits high resistance to loads in the direction of the pile axis. However, flat steel spiral piles twisted around their longitudinal axis have lower bending rigidity and horizontal resistance than steel pipe piles of the same diameter. The authors proposed the foundation structure of batter and vertically-coupled piles with spiral piles with

a depth less than 1 m. The basic resistance characteristics were investigated by model tests and field tests. Previous studies have shown that: 1) Coupled piles have higher horizontal resistance than single piles, and spiral piles have higher horizontal resistance than flat piles.



Fig. 1. Steel spiral pile with flange and pipe (L=950mm).

2) For specimens of the same length, the inclination angle of 45° for the batter pile has the highest horizontal resistance. 3) The Ultimate horizontal bearing capacity depends on the balance between the push-in and pull-out

<sup>1</sup> Manager, Hinode Holdings Co., Ltd, Hinode Global Innovation Center, Saga, 849-0101, JAPAN, t-kurokawa@hinosesuido.co.jp, takeahero21@gmail.com.

<sup>2</sup> Staff, Hinode Holdings Co., Ltd, Hinode Global Innovation Center, Saga, 849-0101, JAPAN, y-ide@hinosesuido.co.jp.

<sup>3</sup> Professor, Geotechnical Engineering Laboratory, Department of Civil Engineering, Faculty of Engineering, Kyushu University, Fukuoka, 819-0395, Japan, yasufuku@civil.kyushu-u.ac.jp.

<sup>4</sup> Section manager, Hinode Holdings Co., Ltd, Hinode Global Innovation Center, Saga, 849-0101, JAPAN, m-nagata@hinosesuido.co.jp.

resistances of the vertical and batter piles, and the ultimate horizontal bearing capacity depends on the weaker of the two (Kurokawa et al. 2021, 2022; Jugdernamjil et al. 2021). The batter and vertically-coupled piles shown in **Fig 2-(a)** are intended to reduce the construction area as much as possible, assuming a narrow environment. This structure is expected to be used as a foundation for vehicle protection fencing at intersections and other locations where construction is limited. Agricultural greenhouses and solar power generation systems also require higher horizontal resistance to repetitive wind loads. However, these facilities are expected to be constructed on large sites. Therefore, the symmetrical batter-coupled piles structure shown in **Fig. 2-(b)** is considered to have a better balance of resistance forces in the axial direction of the pile; and is expected to be more durable against cyclic external forces.

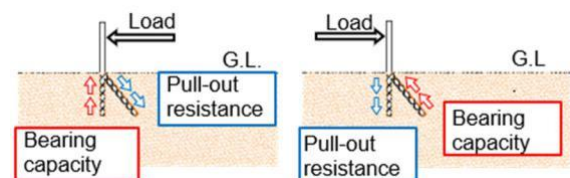
The study of Kuwahara et al. (2004) shows that for symmetrical batter piles coupled with two scaffold pipes, the smaller the inclination angle, the greater the horizontal resistance tends to be. Since a batter pile subjected to horizontal forces rotates the ground around its tip, the authors assume that the smaller the inclination angle of the batter pile, the deeper the tip of the pile and the higher the strength of the ground, which suppresses rotation. Therefore, at an inclination angle of  $45^\circ$ , the penetration depth of the pile becomes shallow, and the pile and sand are pulled up together, thus stagnating the generation of horizontal resistance. The durability of the structure under cyclic loading should also be considered. On the other hand, Goto et al. (1962) observed that increasing the inclination angle of a batter pile greatly increases the horizontal resistance. However, this is only noticeable when the pile tip reaches a strong bearing stratum. Therefore, in their experiments, they used batter-coupled piles with a flat plate with an area of about 10 times the pile cross-sectional area at the tip of a plastic square-bar pile. From the above, it was assumed that the axial resistance of batter-coupled piles is an important factor in achieving horizontal resistance, and that a more compact foundation structure could be achieved by using spiral piles with higher axial resistance to batter piles. However, there have been few studies on the application of spiral piles to batter-coupled piles.

In a previous study, the authors clarified the horizontal resistance characteristics of batter and vertically-coupled pile structures under monotonic loading from a specific direction, but were unable to investigate the durability of the piles under cyclic loading assuming wind loading. In this study, the horizontal resistance of coupled piles consisting of two spiral piles as symmetrical batter-coupled piles (hereafter referred to as "batter-coupled piles" ) is investigated by model tests. To facilitate the

comparison of the effects of the coupled pile configuration and pile shape, a model soil layer was used where the variation of soil conditions can be easily controlled. The soil layer was the same as in the previous study, a dense dry sand, which was considered more likely to exhibit performance differences depending on pile shape. The model piles are mainly spiral batter-coupled piles. For comparison, single piles, coupled piles with two vertical piles (hereafter referred to as "vertically-coupled piles"), "plate batter-coupled piles" with plate piles, and batter-coupled piles with different inclination angles were prepared. Plate piles are assumed to have the shape prior to being processed into the spiral shape. The axial resistance of plate piles is assumed to be less than that of spiral piles, so the effect of the spiral shape is checked.

The purpose of this study is to clarify the effects of batter-coupled piles and vertically-coupled piles, pile shape (spiral and plate), and inclination angle of batter piles on the horizontal resistance characteristics in order to obtain a highly durable coupled pile structure using these model piles. These contribute to the design of more rational and durable foundation structures using spiral piles. Specifically, the method is expected to be applied to foundations for relatively small structures, such as large road signs and agricultural greenhouses, where horizontal loads (mainly wind loads) dominate vertical loads (mainly dead loads).

(a) Batter and vertically-coupled pile structure.



(b) Symmetrical batter-coupled pile structure.

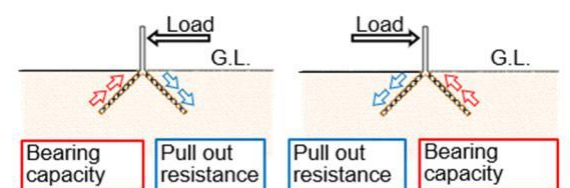


**Fig. 2.** Coupled pile structure and resistance mechanism.

## 2. Experimental Methods

### 2.1 Objectives of the experiment and flow chart

The flow chart of the experiment and the objectives of each experiment are shown in **Fig 3**. The durability under horizontal cyclic loading was evaluated by the magnitude

of the horizontal spring rigidity in the load-displacement relationship of the horizontal cyclic loading experiment. First, the effectiveness of spiral piles in batter-coupled piles and vertically-coupled piles is compared with that of single piles. Next, the effectiveness of spiral piles in the batter-coupled piles is compared with that of plate batter-coupled piles. The inclination angle of the batter pile at which high horizontal spring rigidity can be obtained is then clarified. Finally, cyclic loading tests are performed to evaluate durability.

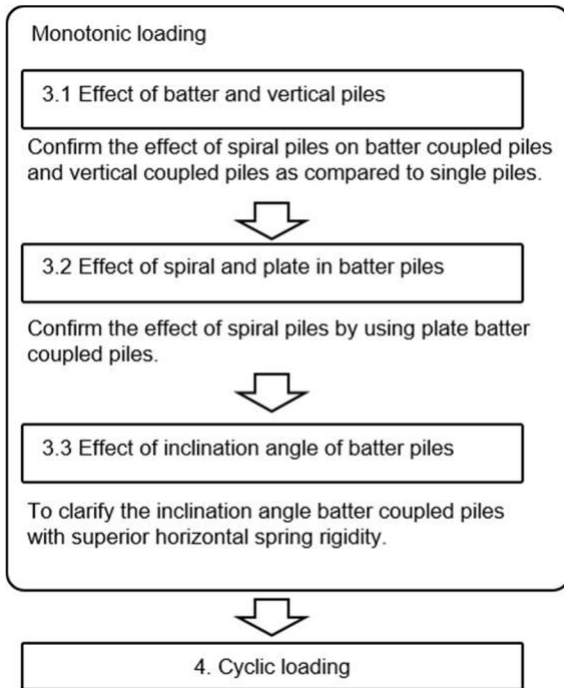


Fig. 3. Experimental flow chart.

## 2.2 Experimental Device Details

The experimental device is shown in Fig. 4. The same test device was used as in the previous study. Tables 1-3 provide an overview of the sand tank, loading device, and instrumentation. The tank is cylindrical with an inner diameter of 750 mm and a depth of 500 mm. Load cells and displacement meters were used to measure the pile head load and the horizontal and vertical displacements of the pile head. The sand used was No. 7 silica sand. The basic and mechanical properties are shown in Table 4, and the results of the triaxial compression tests are shown in Fig. 5-(a), (b), and (c).

The triaxial compression tests were performed under consolidation and drainage conditions using three levels of horizontal stress: 50, 100, and 150 kN/m<sup>2</sup>. The angle of internal friction  $\phi_d$  was obtained by drawing the Mohr stress circle from the test results. The test sand layer was prepared by adding sand to the tank with a bucket seven times and compacting it with a rammer to the specified

depth (approximately 71 mm for one layer), resulting in a relative density of 90%. The sand conditions used in this study were dense, which is considered the most likely condition for the difference in performance between spiral and plate piles.

The model pile was assumed to be driven into the surrounding sand without disturbing it. Sand was placed in the pile with the loader device and pile head connected as shown in Fig. 4. The pile heads were allowed to rotate freely in the vertical direction using a jig. The distance between the tip of the pile and the inner wall of the sand layer was at least five times the pile width  $W$  (=pile diameter, 16mm) for all the model piles to avoid the restraining effect of the tank. The inclination angle of a batter pile is expressed as the angle  $\theta$  from the vertical axis.

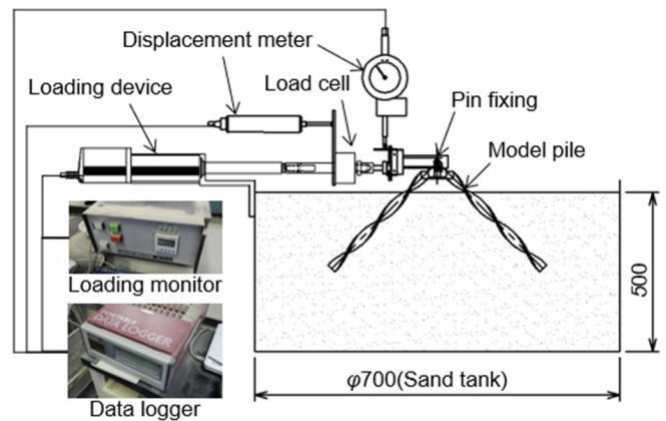


Fig. 4. Experimental device.

Table 1. Sand tank.

Item	Detail	Note
Tank size	$\phi 750 \times h 500$ mm	Columnar tank
Sand type	Silica sand (K-7)	Dry sand

Table 2. Loading device.

Properties	Note
Maximum load	800 (N)
Maximum stroke	50 (mm)
Loading speed	0.01, 0.21 (mm/sec)

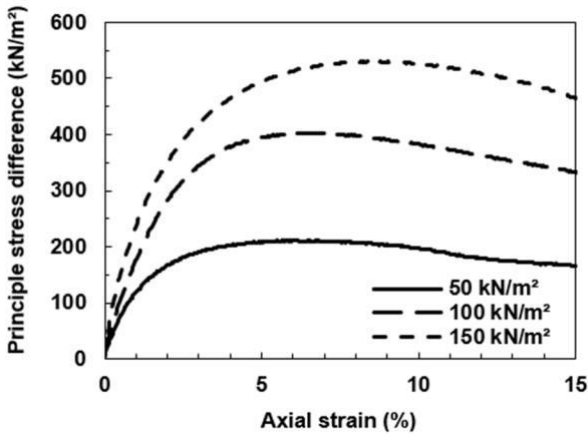
Table 3. Instrumentation.

Item	Capacity
Load cell	1000 (N)
Loading device	50 (mm)
Displacement meter (Horizontal)	50 (mm)
Displacement meter (Vertical)	10 (mm)

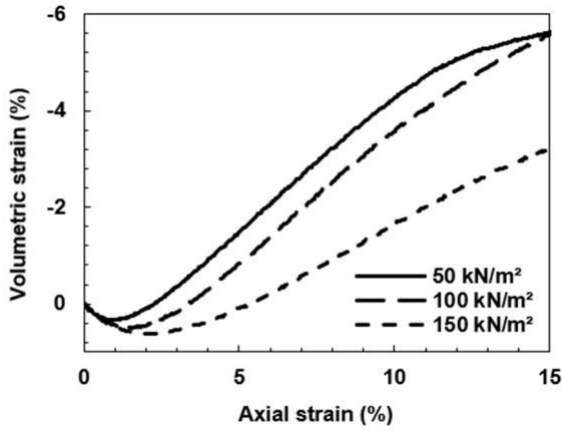
Table 4. Physical and mechanical properties of K-7 sand.

Properties	Value
Specific gravity, $G_s$	2.62
Maximum dry density, $\rho_{max}$	(g/cm <sup>3</sup> ) 1.58
Minimum dry density, $\rho_{min}$	(g/cm <sup>3</sup> ) 1.21
Relative density, $D_r$	(%) 90
Internal friction angle, $\phi_d$ ( $D_r=80$ )	( $^\circ$ ) 37.9

(a) Principal stress difference and axial strain.



(b) Volumetric strain and axial strain.



(c) Mohr's stress circle.

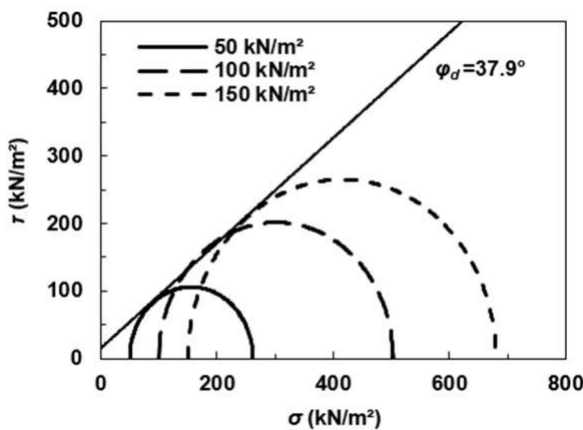


Fig. 5. Triaxial compression test (Consolidated drained).

### 2.3 Model pile

Basic information on the model piles is given in **Table 5**. The plate piles were made directly from flat steel, while the spiral piles were made by twisting the flat steel around its long axis. The length of the model pile was standardized to 216 mm, which is equal to three times the twisting pitch of the spiral. Since the spiral changes its cross-sectional twisted shape when viewed from a fixed direction due to twisting, the second moment of area was calculated in the weak and strong axes. Wang et al. (2019) study that the pitch-width ratio ( $p/W$ ), which is the ratio of the twisting pitch ( $p$ ) of the spiral to pile width ( $W$ ), is superior in balancing the rotational penetration rate and bearing capacity when the ratio is greater than 3.5. In the present study, we used a value of 4.5, which has been used in previous studies by the authors.

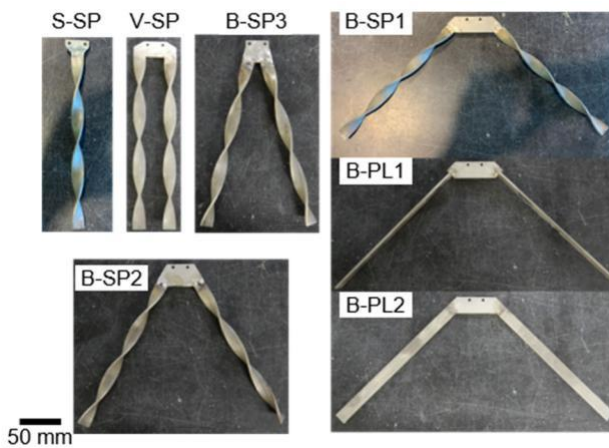
The dimensions of the model pile are shown in **Table 6** and its appearance is shown in **Fig. 6**. The dimensions of the model piles are identical except for the pile head, which is connected to the loading device. The model piles were spiral single piles (S-SP), spiral batter-coupled piles (B-SP1-3), plate batter-coupled piles (B-PL1,2), and spiral vertically-coupled piles (V-SP). Inclination angles for the batter piles were 45, 30, and 15°. Inclination angles of 45° or more were not adopted because of the shallower rooting depth and the difficulty of driving the piles under actual conditions. The vertically-coupled piles were assumed to have a pile center distance of  $2.5W$  ( $=40\text{mm}$ ), which is commonly used in practice, to account for the group pile effect (i.e., the effect of reduced resistance per pile). The rooting depth of the model pile in the sand bed is shorter at larger inclination angles due to the effect of the uniform length of the model pile.

**Table 5.** Properties of model pile.

Parameter	Spiral	Plate
Material		
Young's modulus, $E$	(GPa)	200
The second moment of area,		$I_w$ , Weak axis
$I_w, I_s$	(mm <sup>4</sup> )	36
		$I_s$ , Strong axis
		1,024
Length, $L$	(mm)	216
Width, $W$	(mm)	16
Thickness, $t$	(mm)	3
Twisting pitch, $p$	(mm)	72
Pitch-width ratio, $p/W$		4.5

**Table 6.** Model Pile Specification.

No.	Structure	Pile shape	$\theta$ (°)	$D_p$ (mm)
S-SP	Vertically-single	Spiral	-	182
B-SP1	Batter-couple	Spiral	45	123
B-SP2	Batter-couple	Spiral	30	162
B-SP3	Batter-couple	Spiral	15	187
B-PL1	Batter-couple	Plate (Weak axis)	45	123
B-PL2	Batter-couple	Plate (Strong axis)	45	123
V-SP	Vertically-couple	Spiral	0	182

**Fig. 6.** Appearance of model pile.

### 2.4 Overview of Horizontal Load Tests

Monotonic horizontal loading tests were conducted to verify the horizontal resistance characteristics of the model piles. The loading rate was 0.01 mm/sec by displacement control, and the loading was continuous in one direction. The number of tests was two for each pile, and the load and horizontal displacement of the pile head of the model pile were measured. The test was stopped when the horizontal displacement of the pile head reached the pile diameter (16 mm). From the obtained load-displacement curves, the elastic limit point based on the Weibull distribution curve (hereafter referred to as "yield load:  $P_y$ ") was determined and evaluated for comparison. The determination of yield load by a mathematical method using a Weibull distribution curve has been studied by Okahara et al., (1991) and Nakatani et al., (2003). According to these studies, the method is almost equivalent to the engineering method, in which a load-displacement curve is observed to be the point at which displacement increases rapidly, and is less subject to human error than the engineering method. The equation for the Weibull distribution curve is shown below.

[1]  
The horizontal ultimate bearing capacity estimated by the Weibull distribution curve equation is  $P_{ult}$ , the elastic limit displacement is  $\delta_s$ , and the displacement is  $S$ . Thus,  $P_y$  is the load when the displacement is the elastic limit displacement, so it is expressed by the following equation.

[2]  
The development of the equations and their solutions were obtained in according to with the method proposed by Uto et al., (1982). The maximum load:  $P_{max}$ , horizontal ultimate bearing capacity:  $P_{ult}$ , and yield load:  $P_y$  in the tests were used to compare single piles with batter-coupled piles and vertically-coupled piles, and to evaluate the effects of the shape and inclination angle of the batter-coupled piles.

Finally, cyclic horizontal load tests were conducted on the batter-coupled piles that exhibited the highest horizontal resistance characteristics in the monotonic load tests to verify their durability under cyclic horizontal loads assuming wind loads. Details of the batter-coupled piles tested are described in Chapter 3. The cyclic loading tests were conducted using displacement control at a loading rate of 0.05 mm/sec, with a target of 50 cycles of positive and negative loading. The displacement amplitude was adjusted to apply a pile head load equal to the yield load was applied. Monotonic loading tests were performed after cyclic loading in order to verify the change in horizontal resistance characteristics with and without a cyclic loading history.

### 3. Horizontal resistance characteristics under monotonic loading

The results of the monotonic loading tests and Weibull distribution curves for the maximum load  $P_{max}$ , horizontal ultimate bearing capacity  $P_{ult}$ , yield load  $P_y$ , elastic limit displacement  $\delta_s$ , and horizontal elastic limit spring rigidity (hereafter referred to as spring rigidity)  $k_y$  ( $= P_y/\delta_s$ ) are summarized in **Table 7**. According to Nakatani et al., (2008), when the yield load is determined by the Weibull distribution curve, it is important for the accuracy of the approximation that the pile is of semi-infinite length in order to ignore the horizontal displacement at the pile tip and that the pile body does not yield. The former was not considered a problem since the objective was to compare and evaluate the results. For the latter, it was confirmed that there was no residual deformation of the pile after the test, and it was judged that there would be no problem in applying the method. The test data used for the Weibull



distribution curves were the results up to the maximum load. Details of each result are given in the next section.

**Table 7.** Monotonic loading test results.

No.	$P_{max}$ (N)	$P_{ult}$ (N)	$P_y$ (N)	$\delta_s$ (mm)	$k_y$ (N/mm)
S-SP-1	63.6	63.9	40.4	7.4	5.5
S-SP-2	67.3	79.3	50.1	8.3	6.0
B-SP1-1	108.7	108.5	68.6	0.9	78.2
B-SP1-2	116.4	114.9	72.6	0.9	81.6
B-SP2-1	116.4	114.1	72.1	1.5	49.5
B-SP2-2	110.7	107.7	68.1	1.4	49.3
B-SP3-1	97.8	95.3	60.2	3.3	18.0
B-SP3-2	109.7	107.5	67.9	3.6	19.1
B-PL1-1	72.1	90.8	57.4	10.3	5.6
B-PL1-2	66.1	93.9	59.3	13.4	4.4
B-PL2-1	49.3	66.2	41.8	12.0	3.5
B-PL2-2	54.2	67.1	42.4	10.1	4.2
V-SP-1	102.5	107.2	67.8	5.5	12.3
V-SP-2	111.2	111.7	70.6	5.2	13.7

### 3.1 Effect of batter-coupled and vertically-coupled pile on the horizontal resistance

The horizontal load-displacement curves from the monotonic loading tests of a single pile (S-SP), a batter-coupled pile (B-SP1), and a vertically-coupled pile (V-SP) are shown in **Fig. 7**. The results obtained from the Weibull distribution curves for each type of model pile are also shown in **Fig. 8**, and the yield load of each model pile is indicated by the arrows in **Fig. 7**. The horizontal ultimate bearing capacity determined from the Weibull distribution curve equation was all within 10% of the maximum load in the tests and was considered sufficiently accurate for comparative evaluation. The errors between the measured values and the Weibull distribution curves for individual piles were greater than for the others. This may be mainly due to the fact that the true maximum load is expected to be higher than the test results, as no constant or decreasing trend in the rate of load increase was observed over the test range. Only the batter-coupled piles showed a clear maximum load in the test area. The batter-coupled piles showed a gradual decrease in load and displacement after the maximum load was demonstrated. This is a similar trend to the previous study by Kuwahara et al., (2004).

A comparison of the respective yield loads  $P_y$  and spring rigidity  $k_y$  showed that the batter-coupled piles had the highest yield load and spring rigidity, both about 1.6 times and more than 10 times higher than those of the single pile, respectively, and the same yield load but about 6 times higher spring rigidity than that of the vertically-coupled piles. The resistance of the batter-coupled piles at

0.9 mm (elastic limit displacement) was about 9 times higher than that of the single pile and 4 times higher than that of the vertically-coupled piles. The batter-coupled piles rotated in the ground with the fulcrum near the pile tip and tried to pull out, but the axial push-in support and pull-out resistance of the spiral piles suppressed the rotation, resulting in higher horizontal resistance.

On the other hand, the loads on the monopiles and vertical piles continued to increase as the displacement progressed. The  $P_{ult}$  of the vertically-coupled piles was about 50 N, which was slightly less than twice that of the single pile (about 26 N), and it is assumed that the resistance force was equivalent to that of two piles. It can be concluded that the resistance mechanism of the vertical piles arranged parallel to the load direction is almost the same as that of the single piles. In the aforementioned study by Goto et al. (1962), it was found that the spring rigidity increased rapidly (several to ten times) with increasing inclination angle  $\theta$  for  $0^\circ$  (vertically coupled pile) and  $15^\circ$  and  $30^\circ$  (batter-coupled pile) in a square bar model pile with a flat plate to ensure pile tip resistance. This same tendency was observed in the present experiment, suggesting that the frictional force at the spiral circumference is as effective as the pile tip resistance. In the aforementioned study by Kuwabara et al. (2004), the maximum load of a  $45^\circ$  inclined batter-coupled pile was about 60% of that of a  $0^\circ$  inclined vertically-coupled pile, attributing the shorter rooting depth ( $1/\sqrt{2} \approx 0.7$ ) to the inclination angle. On the other hand, in this experiment, the depth of the batter-coupled pile was about 70% of the depth of the vertically-coupled pile, the same condition as in the previous study, but the maximum loads of the two were equivalent.

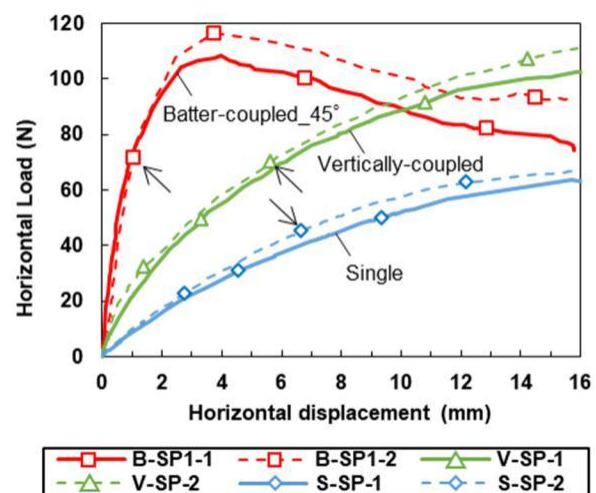
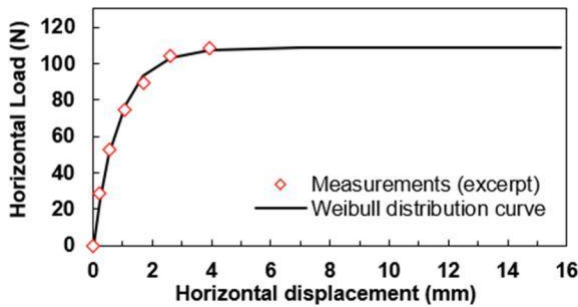


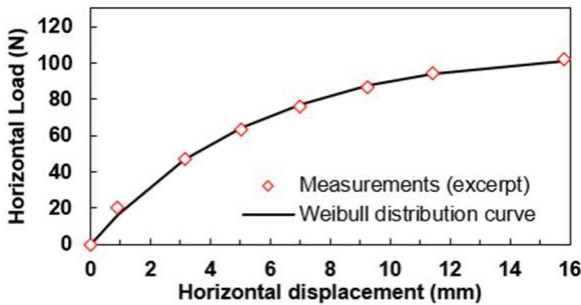
**Fig. 7.** Horizontal load – displacement curves at batter and vertically-coupled piles and single piles.

From the above, it is clear that the batter-coupled pile structure of spiral piles provides better horizontal resistance in the elastic range than the vertically-coupled piles arranged in parallel. It was also suggested that the rooting depth of the pile could be made more efficient. However, when the rooting depth is reduced beyond a certain level, the overlap between the area of the ground that affects the axial resistance of the spiral and the area that affects the horizontal resistance increases, and there is a concern that the subgrade reaction may decrease. It is necessary to clarify the relationship between the horizontal resistance and the spiral by experiments and simulations using the rooting depth as a parameter.

(a) Batter-coupled pile (ex. B-SP1-1).



(b) Vertically-coupled pile (ex. V-SP-1).



(c) Single pile (ex. S-SP-1).

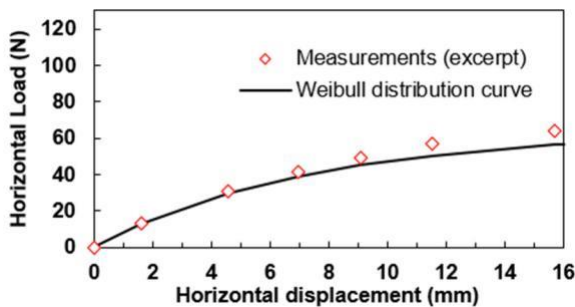


Fig. 8. Weibull distribution curve.

### 3.2 Influence of spiral and plate shape on the horizontal resistance of batter-coupled piles

To verify the effect of pile shape on the horizontal resistance in batter-coupled piles, the load-displacement curves of a batter-coupled pile (B-SP1) and a plate batter-coupled pile (B-PL1,2) are shown in Fig. 9. The yield loads obtained from the Weibull distribution curve equation are also indicated by arrows in the diagram.

The horizontal resistance of the plate batter-coupled piles was lower than that of the batter-coupled piles in terms of both yield load and spring rigidity, especially the spring rigidity was even lower than that of the single piles. The weak axis (B-PL1) had higher resistance than the strong axis (B-PL2). This suggests that the reaction force received from the sand via the lateral area of the pile is more influential than the bending rigidity of the pile body with respect to horizontal forces. In contrast, the fact that there was not much difference in horizontal resistance, even though the lateral area of the pile body was almost twice that of a single pile, is thought to be due to the batter-coupled pile structure. This is thought to be due to the pile body being pulled out by the low axial resistance, causing it to rotate and lift off the ground. In other words, it can be concluded that the higher axial resistance of spiral piles compared to plate piles suppressed the rotation of the pile body, resulting in higher horizontal resistance.

From the above, it is clear that the resistance force in the direction of the pile axis is more important for the horizontal resistance characteristics of batter piles than the bending stiffness of the pile body or the size of the lateral area of the pile body.

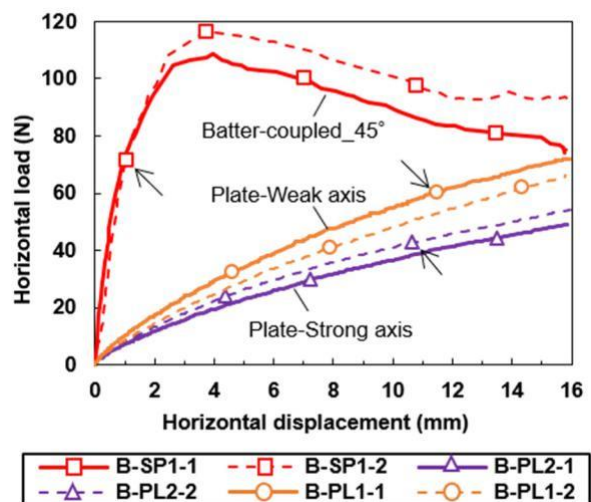


Fig. 9. Horizontal load - displacement curves at spiral batter-coupled and plate batter-coupled piles.

### 3.3 Influence of the inclination angle of the batter-coupled piles on the horizontal resistance

To verify the effect of the inclination angle of the batter-coupled piles on the horizontal resistance, load-displacement curves for B-SP1 to 3 are shown in **Fig. 10**. The yield load obtained from the Weibull distribution curve equation is also indicated by arrows in the diagram. As the inclination angle increased, the yield load and spring rigidity increased and the maximum load was similar. As the inclination angle decreased, it was concluded that the resistance mechanism gradually approached that of vertical piles and single piles, and at an inclination angle of 15°, the resistance characteristics were similar to those of vertically-coupled piles. The horizontal resistance of batter-coupled piles is assumed to consist of the horizontal component of the resisting force in the direction of the pile axis and the subgrade reaction at the side face of the pile body. The 45° inclination angle provided higher horizontal resistance because the horizontal component of the initial axial resistance force was greater than the others. However, when the axial resisting force reached its maximum value, the horizontal resisting force decreased as the displacement progressed. This is probably due to the shallow rooting depth, which reduces the subgrade reaction. Igaue et al. (2006) conducted model tests in dense dry sand using T-shaped model piles with a plate at the tip to ensure the tip bearing capacity of plate batter-coupled piles. Horizontal loading tests were conducted on piles with the same depth of penetration and inclination angles ranging from 0° to 45°. The results showed that the maximum load and spring rigidity increased with increasing angle. The maximum load of the model piles in this experiment remained the same, although the pile rooting depth became shallower as the inclination angle increased. The yield load and spring rigidity increased with increasing inclination angle, showing the same trend. It is suggested that the use of spiral piles for batter-coupled piles may improve pile length efficiency.

According to Goto et al. (1962), the horizontal resistance of batter-coupled piles increases with an increase in the inclination angle  $\theta$ , which affects the horizontal component of the axial resistance force of the batter pile,  $\sin\theta$ . With this as a reference, the relationship between the inclination angle and the horizontal resistance is analyzed focusing on the pull-out pile of the batter-coupled piles. There are two reasons for focusing on pull-out piles. (1) Matsumura et al. (2017) reported how the soil around the piles resisted in model tests of single piles, single batter piles (pull-out piles, push-in piles), and batter-coupled piles using aluminum square pipes through image analysis using X-ray CT. It is shown that the front soil of the push-in piles of batter-coupled piles has the same

subgrade reaction force as that of the single batter piles, while the front soil of the pull-out piles of batter-coupled piles does not have sufficient resistance as a subgrade reaction force against the bending of the pull-out piles. (2) Since relatively short piles were assumed in this experiment, it was assumed that the pull-out resistance would be lower and more dominant than the bearing capacity, considering the fact that a large overburden pressure cannot be expected and the variation in soil conditions near the ground surface. On the other hand, as the inclination angle increases, the rooting depth of the pile becomes shallower and the pull-out resistance is expected to decrease. Murata and Goto (2003) suggested that the pull-out resistance of spiral piles is due to the frictional resistance of the pile circumference plus the shear resistance acting on the conical shear surface created by the engagement with the ground due to the spiral shape. The conical shear failure surface from near the tip of the pile to the ground surface is shown schematically in **Fig. 11** for inclination angle of 45° and 15°.

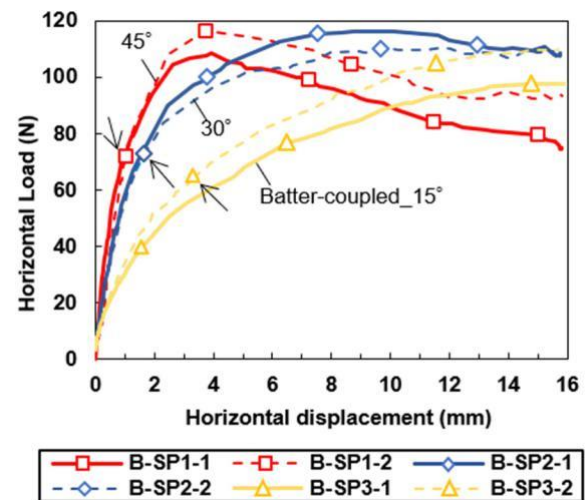


**Fig. 10.** Horizontal load - displacement curves at batter-coupled piles at 15°, 30° and 45° inclination angle.

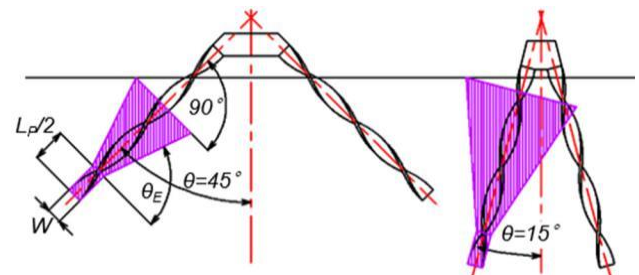


**Fig. 11.** Modeling of the shear failure surface of batter-coupled piles with 15° and 45° inclination angle.



The location of the shear failure surface was considered to be 1/2 pitch (36 mm) from the tip, which is the center of the spiral, with one pitch of the spiral being considered as the anchor section engaging the soil. The apparent pile area at the tip was determined from the pile diameter and added to the shear area.

The angle  $\theta_E$  of the shear surface is reported as  $\varphi$ ,  $90-\varphi$ ,  $90-\varphi/2$ , etc., in relation to the internal friction angle  $\varphi$  of the sand in a previous study of anchor foundations by Ilamparuthi et al. (2002). For the present study,  $90-\varphi_d/2$  ( $= 90-37.9/2 \approx 71^\circ$ ), which has the narrowest shear plane, was chosen for relative comparison. The shear failure surface was considered to be maximum when it reached the sand surface, from which it was determined by partitioning in the direction perpendicular to the pile axis. **Table 8** shows the ratios ( $R\text{-sin}\theta$ ,  $R\text{-}A_s$ ) of  $\sin\theta$  from  $0^\circ$  to  $60^\circ$  inclination angle and shear area with  $45^\circ$  as reference, and the ratio of the two multiplied together ( $R\text{-}H$ ), and compares them with the experimental maximum load ratio ( $R\text{-}P_{max}$ ). The relationship is also shown in **Fig. 12**. The inclination angles of  $30^\circ$  and  $45^\circ$  showed a trend close to the experimental maximum load. The experimental value was 20% higher at an inclination angle of  $15^\circ$ . It is assumed that as the inclination angle decreases, the area where the shear surface overlaps the influence zone on the indentation side increases, which in turn increases the shear strength. From this relationship it can be concluded that the maximum value of horizontal resistance is obtained at an angle of inclination of before and after  $35^\circ$ . However, in the experiments, the yield load and spring rigidity were greatest at  $45^\circ$ . It is suggested that although the shear area contributes to the ultimate limit state, the horizontal component of the pull-out resistance has a greater influence in the elastic region.

The highest spring rigidity was observed at an inclination angle of  $45^\circ$ . The relationship between the horizontal component of the pull-out resistance and the shear area suggests that the peak is reached at about  $35^\circ$ . From the results of this experiment, it can be concluded that the  $45^\circ$  inclination angle with higher spring stiffness is superior in terms of durability performance under cyclic loading.

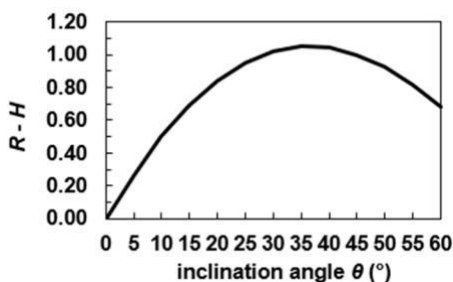


**Fig. 12.** Relationship between the ratio of the horizontal component to the shear area ( $R\text{-}H$ ) and the inclination angle.

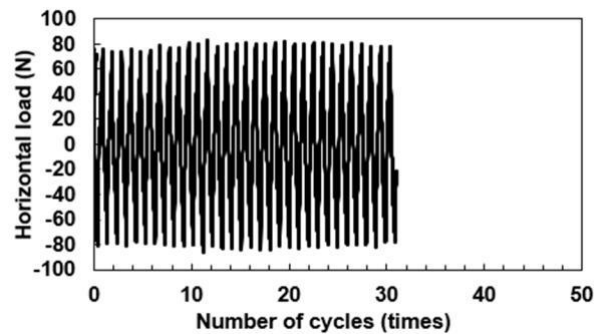
**Table 8.** Relationship between horizontal component of pull-out resistance ( $R\text{-sin}\theta$ ) and shear area ( $R\text{-}A_s$ ) as a function of inclination angle.

$\theta$ ( $^\circ$ )	$R\text{-sin}\theta$	$R\text{-}A_s$	$R\text{-}H$	$R\text{-}P_{max}$
0	0.00	2.32	0.00	-
5	0.12	2.17	0.27	-
10	0.25	2.03	0.50	-
15	0.37	1.88	0.69	0.92
20	0.48	1.73	0.84	-
25	0.60	1.59	0.95	-
30	0.71	1.44	1.02	1.01
35	0.81	1.29	1.05	-
40	0.91	1.15	1.04	-
45	1.00	1.00	1.00	1.00
50	1.08	0.85	0.92	-
55	1.16	0.71	0.82	-
60	1.22	0.56	0.69	-

**4. Horizontal resistance characteristics under cyclic loading**

Based on the results of the previous chapter, a batter-coupled pile (B-SP1) with an inclination angle of  $45^\circ$ , which was judged to have excellent horizontal resistance characteristics, was subjected to cyclic loading tests to verify its durability. The cyclic load - number of cycles is shown in **Fig. 13**.

(a) Cyclic loading at 80 N.



(b) Cyclic loading at 60 N.

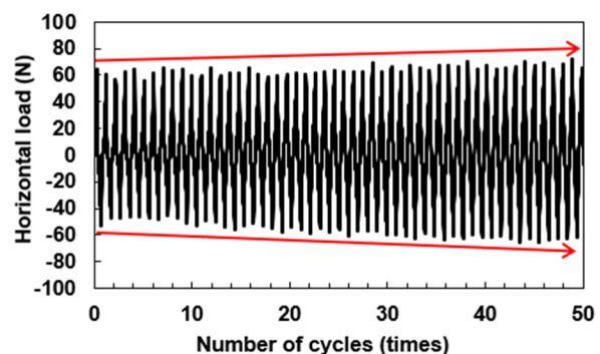


**Fig. 13.** Cyclic horizontal load - Number of cycles.

The load was set as a displacement control using the yield load (about 70 N) as a guide, and two cases were set: 80 N (pile head displacement  $\pm 1.4$  mm), about 15% above the yield load, and 60 N (pile head displacement  $\pm 0.8$  mm), about 15% below the yield load. The load-horizontal displacement curve is shown in **Fig. 14**, and the vertical displacement number of cycles is shown in **Fig. 15**. **Figure 14-(b)** also shows the results of monotonic loading with and without cyclic loading history at 60 N.

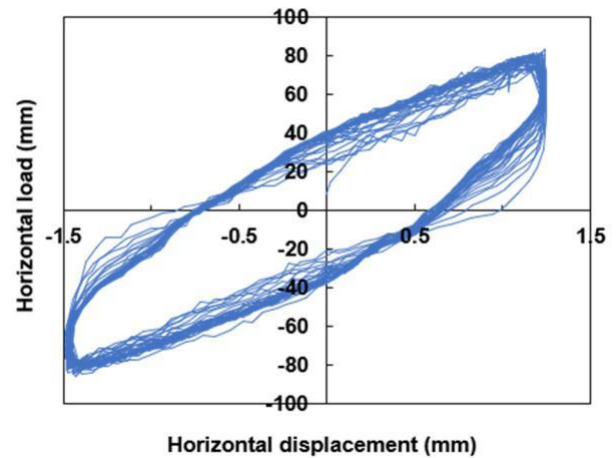
First, the results for a cyclic load of 80 N are discussed. As shown in **Fig. 13-(a)** and **14-(a)**, no change in load was observed after 30 cycles of repeated loading. The reason why the test was terminated after 30 cycles, compared to the target number of 50 cycles, is that the vertical displacement increased proportionally with the number of cycles, as shown in **Fig. 15**, and the test could not be continued because it exceeded the allowable movement of the pile head jig. It can be concluded that when a positive load was applied, the tip of the pile on the rear side lifted up with the tip of the pile on the front side as a fulcrum, and sand flowed into the space created at the same time, and the opposite behavior occurred when a negative load was applied, resulting in the pile gradually lifting up in the vertical direction. This behavior is considered to be more pronounced in the case of dry sand with no adhesive force. Therefore, if the number of cycles is increased, the pile will be pulled out further and the resistance will eventually decrease.

Next, the results at 60N are discussed. As indicated by the arrows in **Fig. 13-(b)**, there was a slight tendency for both positive and negative resistances to increase as the number of cycles increased. The effect of the cyclic loading history is also shown in **Fig. 14-(b)**, where the maximum load is almost the same, but the spring stiffness increases by a factor of 1.5 after cyclic loading. **Figure 15** shows that the increase in vertical displacement was about one-fifth (-80%) that of 80N, which was much smaller than the difference in load value (-30%). The reason for the increase in resistance with cyclic loading is believed to be that sand flowed into a small space around the pile in the direction of loading and was gradually compacted by the cyclic loading. This may be due to the smaller amount of vertical displacement compared to the 80 N case.

The above results confirm that the horizontal resistance of batter-coupled piles does not decrease even when subjected to positive-negative cyclic loading of about 85% of the yield load, and that the piles are durable within the elastic range of the horizontal resistance characteristics. However, since most real environments are assumed to have unsaturated sands, it is difficult for sand to be supplied to the space around the pile by suction and adhesion, and the space may expand more and the resistance may decrease. On the other hand, the amount

of vertical displacement can be suppressed because the dead weight of the superstructure always acts as a dead load in a real environment. This study examined the horizontal resistance of batter-coupled piles, but vertical resistance is also a necessary performance for a foundation. Further studies are needed on the effects of soil conditions, vertical resistance characteristics, and resistance characteristics to combined horizontal and vertical forces.

(a) Cyclic loading at 80 N.



(b) Cyclic loading at 60N and monotonic loading with and without cyclic loading history.

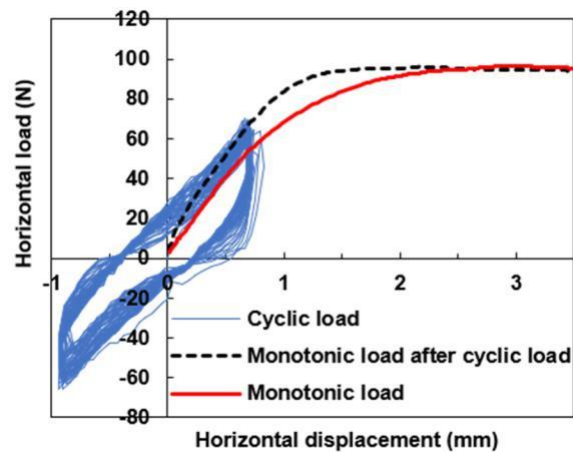


**Fig. 14.** Cyclic horizontal load - displacement curve.

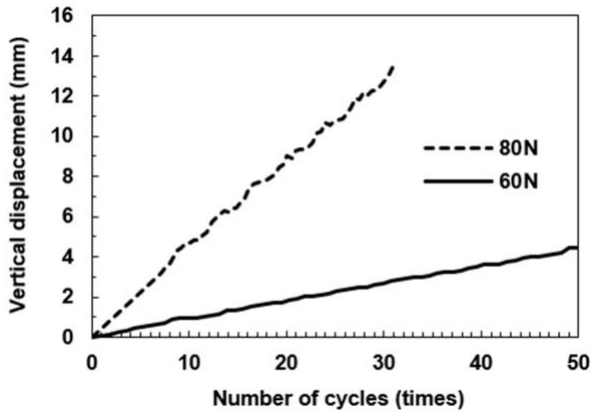


Fig. 15. Vertical displacement - Number of cycles.

## 5. Conclusions

In this study, model tests were mainly conducted to clarify the horizontal resistance characteristics of a coupled pile structure in dense sand using spiral piles as batter piles. The results were analyzed in terms of the effects of batter-coupled and vertically-coupled piles, pile shape (spiral and plate), inclination angle of the batter-coupled piles, and durability of the coupled piles under horizontal cyclic loading. The major results and findings are summarized below.

- 1) The coupled pile structure with two batter piles using spiral piles (hereafter referred to as "batter-coupled piles") showed higher spring rigidity and yield load than the single pile and the vertically-coupled pile with two spiral piles.
- 2) In batter-coupled piles, spiral piles had higher spring stiffness and yield load than plate batter-coupled piles. The results showed that the horizontal resistance of batter-coupled piles was more important than the rigidity and lateral area of the pile body, and revealed the usefulness of spiral piles in batter-coupled piles.
- 3) For inclination angles of 15, 30, and 45° for batter-coupled piles, the pile with 45° inclination angle was found to have the highest spring rigidity. On the other hand, the relationship between the horizontal component of the pull-out resistance and the shear area suggests that the horizontal ultimate bearing capacity is obtained at about 35°.
- 4) The durability of the 45° inclination angle batter-coupled piles was confirmed by cyclic loading tests at a load equal to 85% of the yield load in dense sand.
- 5) For the rational design of batter-coupled piles with spiral piles, it is necessary to study the resistance characteristics under realistic soil conditions, the

vertical bearing capacity characteristics, and the resistance characteristics to combined horizontal and vertical forces.

## References

- Goto, H., and Ashimi, T., Takii, T. 1962. Model teste and their considerations about horizontal resistance of batter piles and combined piles. *JSCE*, **79**: 24-34. (in Japanese)
- Ilamparuthi, K., and Dickin, E. A., Muthukrisanaiah, K. 2002. Experimental investigation of the uplift behaviour of circular plate anchors embedded in sand. *Canadian Geotechnical Journal*, Vol. 39, Issue.3, p.648-664, 2002.
- Jugdernamjil, A. and Yasufuku, N., Kurokawa, T., Tani, Y., Nagata, M. 2021. Experimental observation on the ultimate lateral capacity of vertical-batter screw pile under monotonic loading in cohesionless soil. *Proc. 2<sup>nd</sup> International Press-in Engineering (ICPE2021)*, Kochi, Japan: 158-165.
- Kurokawa, T., and Tani, Y., Nagata, M., Jugdernamjil, A., Yasufuku, N. 2021. A study on analysis of horizontal resistance of screw coupled foundation with vertical and battered piles in cohesionless soil. *Proc. 2<sup>nd</sup> International Press-in Engineering (ICPE2021)*, Kochi, Japan: 172-182.
- Kurokawa, T., and Yasufuku, N., Ide, Y., Nagata, M. 2022. Horizontal resistance of screw coupled foundation with vertical and battered piles in sandy ground. *The 57<sup>th</sup> Geotechnical Research Presentation*, (in Japanese).
- Kuwabara, T., and Kimata, T., Kudo, Y., Yamagata, T., Kitajima, H. 2004. A Study on horizontal loading characteristics of batter piles as a greenhouse foundation. *Sci. Rep. Grad. Sch. Agric. & Biol. Sci., Osaka Pref. Univ.* 56: 23-28 (2004). (in Japanese)
- Kuwamura, H., and Sato, Y. 2015. Strength and Stiffness of Thickened Non-Diaphragm CHS to H-Beam Connection. *J. Struct. Constr. Eng., AIJ*, Vol. **80** No. 716, 1611-1619, Oct., 2015. (in Japanese)
- Murata, S., and Goto, T. 2003. Vertical loading and pulling tests of spiral piles in the field. *Japanese Geotechnical Society, Soils and Foundations*, **51** (11): 11-13, Nov., 2003.
- Nakatani, S., and Shirato, M., Iochi, H., Matsui, K. 2008. Geotechnical criterion for elastic limit of horizontally – loaded deep foundations. *JSCE*, Vol. **64** No. 3, 616-628, Aug, 2008. (in Japanese)
- Okahara, M., and Takagi, S., Nakatani, S., Kimura, Y. 1991. A study on bearing capacity of single pile and design method of column type of foundation. Technical

Memorandum of PWRI (2919), Public Works Research Institute. (in Japanese)

Uto, K., and Fuyuki, M., Sakurai, M. 1982. Organizing result of pile load test, *Foundation Engineering & Equipment, Monthly*, **10** (9): 21-30, Sep, 1982.

Wan, Q., and Jugdernamjil, A., Yasufuku, N., Ishikura, R., Alowaisy, A., Kurokawa, T., Ide, Y., Nagata, M. 2022. Behavior of lateral resistance of spiral pile in sandy ground under cyclic loading. *Japan Society of Civil Engineers 2022 Annual Meeting*, (in Japanese).

Wang, K., and Tani, Y., Yasufuku N., Ishikura, R., Fujimoto, H. & Nagata, M. 2019. Bearing capacity characteristics of the spiral pile in sandy ground focused on pitch-width ratio. *The 54<sup>th</sup> Geotechnical Research Presentation*, (in Japanese).

### Symbols and abbreviations

$A_s$	Shear area
$D_r$	Relative density
$D_P$	Depth of pile
$E$	Young's modulus of model pile
$G_s$	Specific gravity
$I_s$	Strong-axis of the second moment of area of model pile
$I_w$	Weak-axis of the second moment of area of model pile
$K_y$	Horizontal elastic limit spring rigidity
$L$	Length of model pile
$L_P$	Length of twisting pitch
$P_{max}$	Horizontal maximum load
$P_{ult}$	Horizontal ultimate bearing capacity
$P_y$	Horizontal yield load
$t$	Model pile thickness
$W$	Width of model pile
$\delta_s$	Elastic limit displacement
$\theta$	Inclination angle of battered pile
$\theta_E$	Shear failure angle
$\rho_{max}$	Maximum dry density
$\rho_{min}$	Minimum dry density
$\sigma$	Principal stress
$\tau$	Shear strength
$\varphi_D$	Internal friction angle